

## EXPERIMENTAL VALIDATION OF A MULTI-DIMENSIONAL POPULATION BALANCE MODEL INCORPORATING BREAKAGE, IN HIGH-SHEAR MIXER GRANULATION

R. Ramachandran <sup>a</sup>, C.D. Immanuel <sup>a\*</sup>, F. Stepanek <sup>a</sup>, J.D. Litster <sup>b</sup>, F.J. Doyle III <sup>c</sup>

<sup>a</sup> Department of Chemical Engineering and Chemical Technology, Imperial College London,  
Exhibition Road, London SW7 2AZ, United Kingdom; e-mail: c.immanuel@imperial.ac.uk

<sup>b</sup> School of Chemical Engineering, Purdue University, West Lafayette, IN 47907-2100, United  
States of America

<sup>c</sup> Department of Chemical Engineering, University of California at Santa Barbara, Santa  
Barbara, CA 93106-5080, United States of America

**Abstract.** In this study, a dynamic model is presented for the granulation process, employing a three-dimensional population balance framework. The major focus of this work is the development and experimental validation of a novel mechanistic breakage kernel that is incorporated within the population balance equation. Qualitative validation of breakage kernel/model was first performed and trends of lumped properties (i.e., total particles, average size, binder content and porosity) and distributed properties (i.e., granule size and fractional binder content) show good agreement with the expected phenomenological behaviour. Successful high-shear mixer granulation experiments using glass-ballotini as the powder and poly-vinyl alcohol in water (PVOH-H<sub>2</sub>O) as the liquid binder were then carried out to mimic predominantly breakage only behaviour whereby the rate of breakage was greater than that of nucleation and aggregation. Good agreement between experimental and simulation results were obtained for the granule size distribution under different operating conditions. In addition, accurate model predictions were obtained for the evolution of the lumped properties.

**Key words:** Granulation, High-shear mixing, Multi-dimensional Population Balance, Breakage, Mechanistic kernels, Experimental validation

### 1. INTRODUCTION

Granulation is a particle production process of converting fine powdery solids into larger free-flowing agglomerates. It finds application in a wide range of industries (*e.g.* pharmaceuticals, fertilisers and minerals) as granulated products often have notable improvements compared to their ungranulated form. However, industrial granulation processes are by-and-large operated in a highly inefficient manner with large recycle ratios within the process (3-4:1, recycle/product) [1]. Therefore, an integrated systems modelling approach will be a crucial aid to mitigate this situation [1,2]. Furthermore, a comprehensive model of the process will enable an analysis of the system dynamics and the formulation of a suitable control strategy, which potentially could contribute to a more efficient operation of the process [1,2].

Granulation can be viewed as a combination of only three phenomenological rate processes: wetting and nucleation, consolidation and growth, and attrition and breakage [3]. The formation of granules is first initiated by the nucleation of fine powder (primary particles). The nuclei particles will continue to grow via aggregation and consolidation as they collide with other (nuclei) particles and the walls of the granulator. Granule breakage may also result due to collisions. Previously, a methodology for the aggregation and nucleation mechanistic kernels has been developed and validated [4-6]. The impetus behind the current study is to validate a three-dimensional population balance model incorporating a mechanistic kernel for the breakage phenomenon in combination with a simple empirical function for consolidation. This is carried out by performing batch granulation experiments for a Ballotini-Polyvinyl alcohol in water (PVOH-H<sub>2</sub>O) granulation recipe and measuring granule evolution with respect to particle size, fractional binder content and porosity. Similar to the breakage only experiments performed by Liu et al. (2008) [7], experiments were designed such that the rate of breakage was greater than the rates of nucleation and aggregation so that a breakage-consolidation only model was utilized for experimental validation.

## 2. MECHANISTIC MODEL

The granulation process can be modelled using population balance equations (PBEs) accounting for the individual rate processes. The breakage kernel is a very important component in the population balance model, as breakage of wet granules will control the final granule size distribution. In some cases, breakage can be used to limit the maximum granule size or help distribute a viscous binder [3]. Due to the limited knowledge of the mechanisms that underlie the granulation process, most of the proposed breakage kernels are empirical or semi-empirical in nature and have been largely formulated based on experimental observations. Therefore, in order to further improve the predictive capabilities of the breakage models and to extend their region of validity, one has to directly incorporate the mechanistic features of the process and develop a kernel strongly based on first principles. Such kernels are also useful when it comes to scale-up of processes. A three-dimensional population balance model employed in a previous study for modelling the granulation process which considers aggregation, nucleation and consolidation is employed in this work [4-6]. A multi-dimensional model is warranted as previous studies have shown evidence of heterogeneity during high-shear granulation [8,9]. In the present model, the particle population distribution is tracked according to the particle size, binder content and porosity, which are then recast in terms of the volume of solid (*s*), volume of liquid (*l*) and volume of gas (*g*) to facilitate the formulation of the three-dimensional PBE in Equation (1),

$$\begin{aligned} \frac{\partial}{\partial t} F(s, l, g, t) + \frac{\partial}{\partial g} \left( F(s, l, g, t) \frac{dg}{dt} \right) &= \mathfrak{R}_{break} \\ &= \int_s^\infty \int_l^\infty \int_g^\infty K_{eff}(s_1, l_1, g_1) b(s, l, g, s_1, l_1, g_1) F(s_1, l_1, g_1, t) - K_{eff}(s, l, g) F(s, l, g, t) \end{aligned} \quad (1)$$

In Equation (1),  $F(s, l, g, t)$  represents the population density function defined such that  $F(s, l, g, t) ds dl dg$  is the moles of granules of solid volume between  $s$  and  $s + ds$ , liquid volume between  $l$  and  $l + dl$ , and gas volume between  $g$  and  $g + dg$ . The partial derivative term with respect to  $g$  accounts for the consolidation phenomenon. During consolidation granules experience a reduction in pore volume and an increase in the liquid saturation as there is only a decrease in the pore volume but the volume of solid and liquid remain

unchanged. The consolidation phenomenon accounts for the densification of the granules and the associated reduction in the particle porosity (modelled using an empirical relation as shown where the constant  $c$  is dependent upon the mixing rate in the granulator) [10].  $\mathfrak{R}_{break}$  represents the rate of breakage,  $K_{eff}$  is the breakage kernel and  $b$  is the breakage function, which has previously been developed [11]. In solving this three-dimensional population balance model, a hierarchical solution strategy is employed [5].

## 2.1 Breakage Kernel

The breakage kernel is modelled as a quotient of applied external stress ( $\sigma_{ext}$ ) on a granule over innate strength ( $\sigma_{in}$ ) of a granule, where  $A$  is a proportionality constant. Refer to Equation (2).

$$K_{break} \propto \frac{\text{external stress}}{\text{innate strength}} = A \times \frac{\sigma_{ext}}{\sigma_{in}} \quad (2)$$

The external stress in turn is calculated from the external forces over their contact area. These external forces are a result of (i) fluid forces in the granulator, (ii) particle-particle collisions and (iii) particle-wall collisions. For cases (i) and (iii) the breakage kernel is defined as in Equation (3).

$$K_{break}(s, l, g) = A \times \frac{\sigma_{ext}(s, l, g)}{\sigma_{in}(s, l, g)} \quad (3)$$

Where,  $s$ ,  $l$  and  $g$  are the solid, liquid and gaseous volumes of an  $i^{\text{th}}$  particle. For case (ii) the breakage kernel is defined as in Equation (4).

$$K_{break}(s, l, g, s_1, l_1, g_1) = A \times \frac{\sigma_{ext}(s, l, g, s_1, l_1, g_1)}{\sigma_{in}(s, l, g)} \quad (4)$$

Where,  $s_1$ ,  $l_1$  and  $g_1$  are the solid, liquid and gaseous volumes of a  $j^{\text{th}}$  particle. The intrinsic strength of the granule is derived from the capillary, viscous and frictional forces (incorporated in  $\sigma_{in}$ ) that are responsible for the liquid bridge strength of the granule [12] in addition to the cohesive strength between solid particles. Subsequently the individual breakage kernels for the three types (i-iii) of breakage are transformed into an effective breakage kernel that is based on the probability of an  $i^{\text{th}}$  size particle colliding with another particle of  $j^{\text{th}}$  size, or a wall. Fluid forces act in addition to forces (ii) and (iii). Refer to Equation (5).

$$K_{eff}(s, l, g) = A \times \sum_{s_1=1}^m \sum_{l_1=1}^n \sum_{g_1=1}^o \left[ \frac{\sigma_{ext}(s, l, g, s_1, l_1, g_1)}{\sigma_{in}(s, l, g)} \right] \times F(s_1, l_1, g_1) \times N_a \quad (5)$$

$$\times \frac{SA(s_1, l_1, g_1)}{TSA + WA} + \left[ \frac{\sigma_{ext}(s, l, g)}{\sigma_{int}(s, l, g)} \times \frac{WA}{TSA + WA} \right]$$

Where,  $F$  is the particle density;  $WA$  is the total wall area within the granulator;  $TSA$  is the total particle area;  $SA$  is the individual particle area;  $N_a$  is Avogadro's constant;  $m$ ,  $n$  and  $o$  correspond to the breakage size upper limits. A complete derivation of the breakage kernel is available in Ramachandran (2008) [13].

### 3. MATERIALS AND METHODS

For the high-shear mixer granulation experiments, glass-ballotini was used as the primary powder. This material had a mass mean diameter of 112  $\mu\text{m}$  and a size range of 75 -150  $\mu\text{m}$ . The skeletal density of the material was 2.48  $\text{kg}/\text{m}^3$ . Polyvinyl alcohol (PVOH) in water (2.5% and 5% concentration by mass) was used as the liquid binder. For each high-shear experiment, approximately 250 g of dry powder was used to form larger wet granules. These granules were then sieved and granules within the 500 - 600  $\mu\text{m}$  size range were then used as the starting material to perform the breakage only granulation experiments. Due to limited amount of residual binder, the rate of breakage was greater than the rates of nucleation and aggregation. After drying, the granule size distribution (GSD) was determined via a particle size and shape analyser (Ankersmidt). An average binder content at different sampling times was measured by means of thermo-gravimetry. In a similar fashion, the average porosity was determined by means of pycnometry.

### 4. RESULTS AND DISCUSSION

#### 4.1 Breakage Kernel Simulation Results

Figures 1a-c depict the simulated shape of the breakage kernel (Equation 5) with respect to two dimensions (i.e., solid-liquid, solid-gas or liquid-gas) keeping the third dimension constant (i.e., solid, liquid or gas). The shapes observed are in agreement with expected phenomenological behaviour. In Figure 1a for a very small liquid content and constant gas volume, we see that  $K_{\text{eff}}$  decreases marginally as solid volume increases. This is attributed to the fact that at very low liquid contents, the strength of the bond is mainly due to the cohesive strength between solid particles. Hence increase in solid volume increases the cohesive strength. For the case of a large liquid content,  $K_{\text{eff}}$  increases as solid volume increases. This is because, in the current case, the strength of the bond is mainly due to the liquid bridges and as solid volume increases, the liquid bridge strength decreases. The sharp peak seen in the figure as solid volume and liquid volume approach zero is due to negligible solid cohesive forces and liquid bridge forces that result in an exponential increase in  $K_{\text{eff}}$ . In Figure 1b we see that there is an increase in  $K_{\text{eff}}$  as both solid and gas volumes increase. This is due to the fact that at a constant liquid volume, these increases cause the liquid bridge strength to decrease significantly. In Figure 1c we see that there is an increase in  $K_{\text{eff}}$  as liquid volume decreases and gas volume increases. This is because liquid directly affects the liquid bridge strength and gas volume adversely affects the liquid bridge strength.

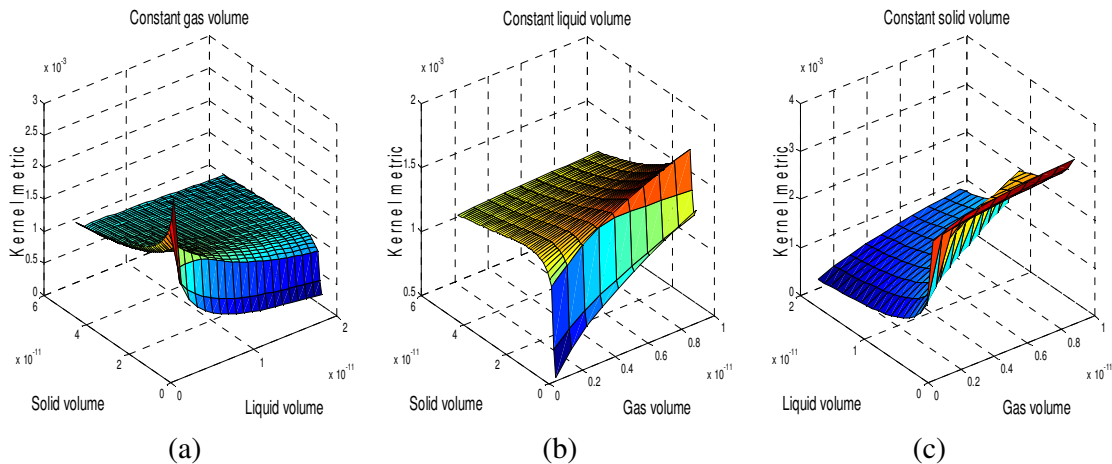


Figure 1: Shape of the kernel with respect to 2 dimensions keeping the 3<sup>rd</sup> dimension constant.

## 4.2 Model Validation Results

The population balance model was validated by comparing the simulated output with experimental measurements. Granule samples were taken out from the drum granulator at intermittent time intervals at time instances of 60s, 120s, 240s and 600s. In the model, the primary particles are monodispersed with an average diameter of 550  $\mu\text{m}$ . Other model inputs such as the initial number of seed particles, binder viscosity, binder surface tension and particle shape factor were set accordingly as per actual experimental conditions. A sensitivity analysis around the nominal operating regime was performed to determine the influence of the model inputs on the final output (particle density). Based on this analysis, sensitive parameters such as breakage size limits,  $c$  (Equation 25 in [9]) and  $A$  (Equation 5) were used as tuning parameters for matching the predicted model outputs with experimental measurements of the granule attributes. The first set of data (case 1) was used to tune the model i.e., estimate the parameters in the model. Subsequently, the tuned model was used to predict the GSD and evolution of average diameter at a different operating condition/formulation (case 2). In the present study, Case 1 corresponds to a binder viscosity of 0.0052 Pa.s (2.5% PVOH-H<sub>2</sub>O) and case 2 corresponds to a binder viscosity of 0.022 Pa.s (5% PVOH-H<sub>2</sub>O). The parameters,  $c_1$  ( $5 \times 10^{-5}$ ) and  $A$  ( $1.5 \times 10^{-9}$ ) were used in both cases. The model was tuned by increasing or decreasing one of the sensitive parameters while holding the others constant. For instance, if the rotational speed of the mixer is changed, the tuning parameters would remain the same, but  $u_0$  (model parameter in the breakage kernel, indicating rotational speed) will be updated to the new value. This applies to other material and process variables. In this manner, the breakage kernel (upon successful prediction of granule dynamics at other operating conditions) can be utilised as a predictive model which would be useful for design, scale-up, operation and control.

Figure 2a depicts the simulated temporal evolution of the total particles in the system which increases due to particle breakage, for cases 1 and 2. It can be seen that the rate of breakage increases with time and this is attributed to the geometrical progression of particle breakage. Due to the higher binder viscosity in case 2, the liquid bridge strength is higher which in turn slows down the rate of breakage compared to case 1. Figure 2b shows the change in average particle diameter with time. The model is able to capture the particle level phenomena and sensitivities of the process resulting in a close match between the simulated profile and experimentally measured data for both cases. Due to the higher liquid bridge strength, average particle diameter for case 2 is higher than that of case 1. Figures 2c and 2d depict the change in average porosity and binder content with time respectively, for case 1. It can be seen that within acceptable measurement error, the model is able to capture the range of these average properties. Average binder content reported remains constant throughout as no binder is added or removed to/from the system. A marginal increase is observed for average porosity and this attributed to the consolidation effect not strong enough as compared to particle breakage, to effect any decrease in particle porosity. Similar observations were obtained for case 2 (Figures not shown).

Figures 3a-d and 4a-d show the GSD model and experimental profiles at each time instance corresponding to the intermittent sampling times (i.e., 60s, 120s, 240s and 600s) during the experiment for cases 1 and 2 respectively. The GSDs are represented as the normalised volume frequency ( $V_f$ ) of granules with respect to granule diameter ( $D$ ) (i.e.,

$$V_f(D,t) = \frac{F(D,t)}{\int F(D,t)dD} \times \frac{V(D)}{\int V(D)dD}, \text{ where } V \text{ is the particle volume. A clear progression is}$$

observed during the course of granulation whereby particles undergo breakage forming

smaller sized particles, which is depicted by a gradual reduction in the peak corresponding to 550  $\mu\text{m}$ . It can be seen that the tuned model is able to accurately capture the experimental GSD for case 1 and thereafter able to accurately match/predict accurately the GSD for case 2. Figure 5 depicts the end-point 2D distribution of total particle numbers with respect to particle diameter and fractional binder content. As seen in the plots, the particles in the initial seed undergo breakage to form a smaller mode of particles with a larger distribution width. More experimental cases are presented in Ramachandran (2008) [13], for which the model is validated at different operating conditions and formulations.

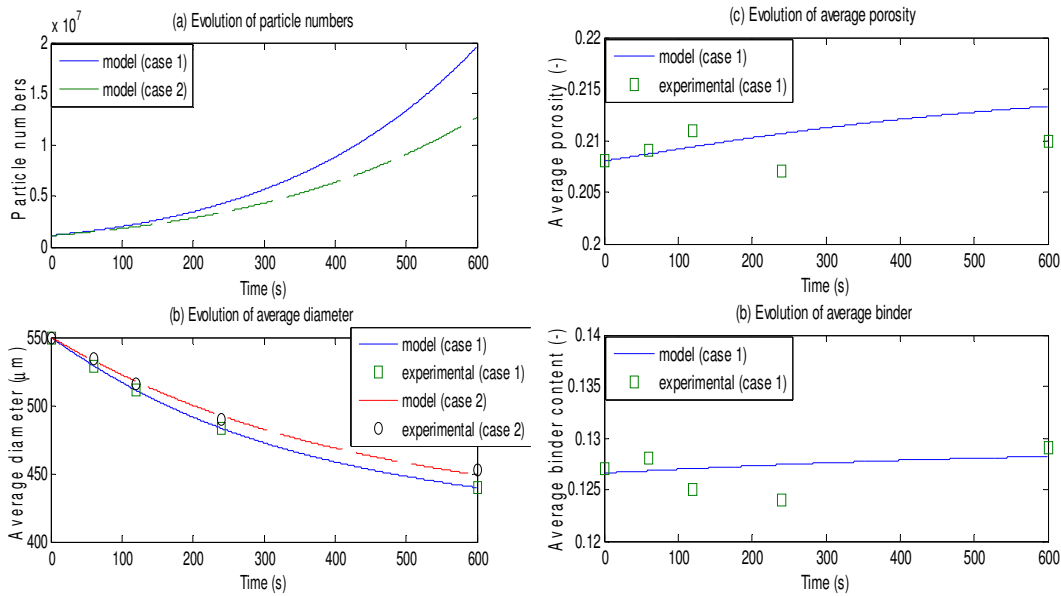


Figure 2: Evolution of temporal profiles for (a) particle numbers, (b) average diameter, (c) average porosity and (d) average binder content.

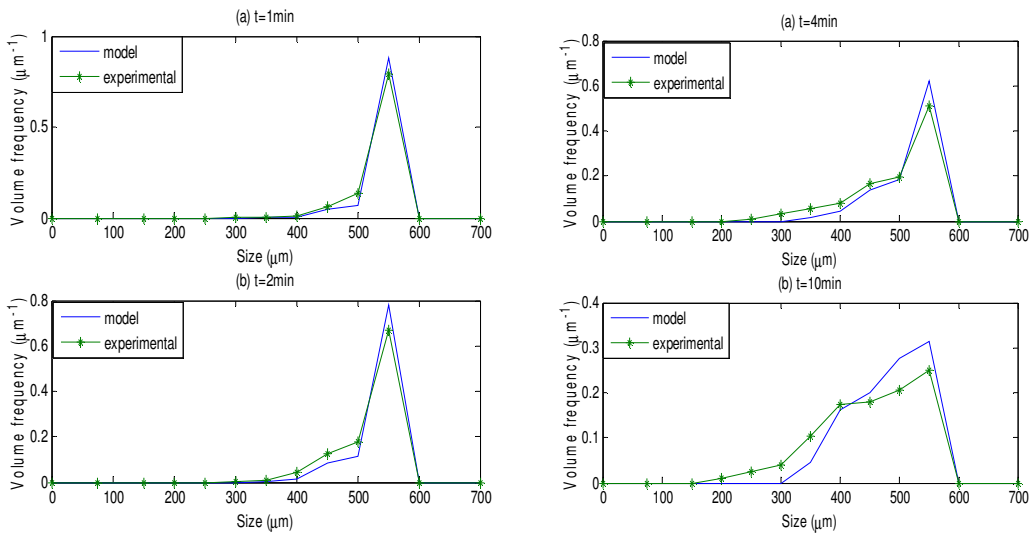


Figure 3: Comparison between simulations and experimental data for time profiles of GSDs for case 1.

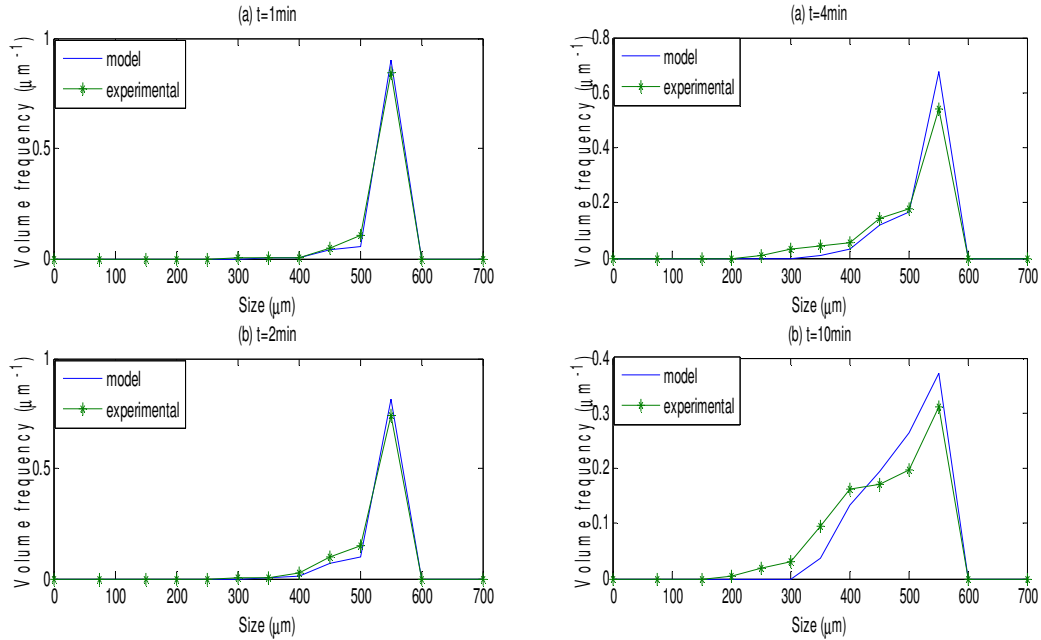


Figure 4: Comparison between simulations and experimental data for time profiles of GSDs for case 2.

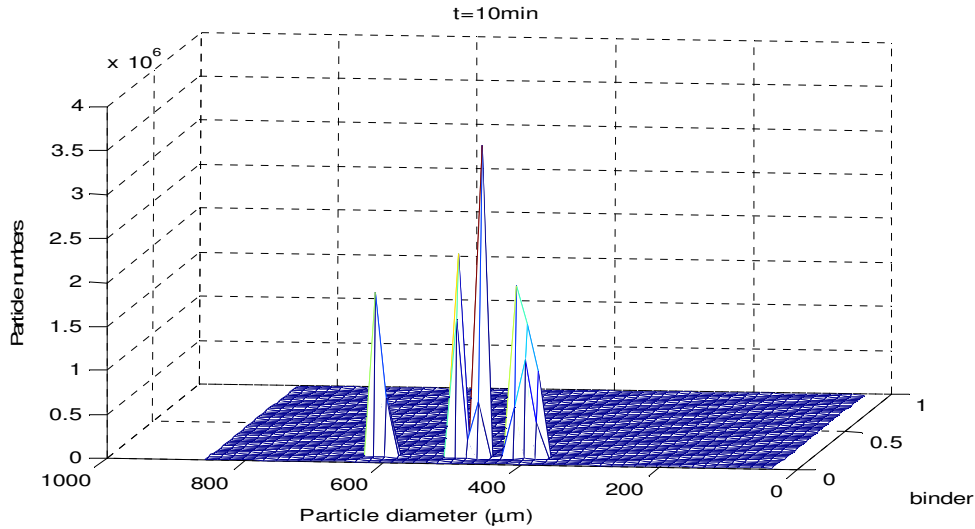


Figure 5: End-point ( $t=10$  min) 2D distribution across size and fractional binder content.

## 5. CONCLUSIONS

The three-dimensional population balance model employing a mechanistic representation for the breakage phenomenon was validated for a ballotini/PVOH-H<sub>2</sub>O recipe. Lab-scale experiment and data analyses were performed to obtain averages/distributions of size, binder content and porosity. Qualitative validation of the breakage kernel was performed and resulting kernel shapes show good agreement with the expected phenomenological behaviour. Successful experiments were performed to mimic predominantly breakage only behaviour whereby the rate of breakage was greater than that of growth enhancing mechanisms such as nucleation and aggregation. Quantitative validation of the GSDs between the model predictions and those obtained in experiments for both cases showed very good agreement.

The model predictions for the average properties (i.e., size, binder content and porosity) were in close agreement to the experimentally measured data. These results are promising toward a comprehensive first-principles predictive model for the granulation process, that can help reduce large number of experiments.

## 7. REFERENCES

1. Mort P.R., 2005. "Scale-up of binder agglomeration processes", *Powder Technology*, **150**, 86-103.
2. Bardin M., Knight P.C., Seville J.P.K., 2004. "On control of particle size distribution in granulation using high shear mixers", *Powder Technology*, **140**, 169-175.
3. Iveson S.M., Litster J.D., Hapgood K., Ennis B.J., 2001 "Nucleation, growth and breakage phenomena in agitated wet granulation processes: a review", *Powder Technology*, **117**, 3-39.
4. Immanuel C.D., Doyle III F.J., 2005. "Solution technique for a multi-dimensional population balance model describing granulation processes", *Powder Technology*, **156**, 213-225.
5. Poon J., Immanuel C.D., Doyle III F.J., Litster J.D., 2008. "A three-dimensional population balance model of granulation with a mechanistic representation of the nucleation and aggregation phenomena", *Chemical Engineering Science*, **63**, 1315-1329.
6. Poon J., Ramachandran R., Sanders C.F.W., Glaser T., Immanuel C.D., Doyle III F.J., Litster J.D., Wang F.Y., Cameron I.T., 2008. "Experimental Validation Studies on a Multi-Dimensional and Multi-Scale Population Balance Model of Batch Granulation", *Submitted to Chemical Engineering Science*.
7. Liu L.X., Smith. R., Litster J.D., 2008. "Wet granulation breakage in a breakage only high shear-mixer: Effect of formulation properties on breakage behaviour", *Accepted to Powder Technology*.
8. Scott A.C., Hounslow M.J., Instone T., 2000. "Direct Evidence of Heterogeneity during High-Shear Granulation", *Powder Technology*, **113**, 205-213.
9. Biggs C.A., Sanders C., Scott A.C., Willemse A.W., Hoffman A.C., Instone T., Salman A.D., Hounslow M.J., 2003. "Coupling granule properties and granulation rates in high-shear granulation", *Powder Technology*, **4626**, 1-7.
10. Verkoeyen D., Pouw G.A., Meesters G.M.H., Scarlett B., 2002. "Population balances for particulate processes -- a volume approach", *Chemical Engineering Science*, **57**, 2287-2303.
11. Pinto M.A., Immanuel C.D., Doyle III F.J., 2007. "A feasible solution technique for higher-dimensional population balance models", *Computers and Chemical Engineering*, **31**, 1242-1256.
12. Iveson S.M., Beathe J.A., Page N.W., 2002. "The dynamic strength of partially saturated powder compacts: the effects of liquid properties", *Powder Technology*, **127**, 149-161.
13. Ramachandran, R., 2008. "Multi-scale population balance modelling and controllability of granulation processes", PhD Thesis, Imperial College London, *In Preparation*, 2008.